Electronic Supplementary Material (ESI) for Journal of Materials Chemistry B.
This journal is © The Royal Society of Chemistry 2023

Supplementary information

Validation of transparent and flexible neural implants for simultaneous electrophysiology, functional imaging, and optogenetics

Lina Koschinski[a,b,c], Bohdan Lenyk†, Marie Jung[a,c], Irene Lenzi[a,c], Björn Kampa[c,d], Dirk Mayer[a], Andreas Offenhäusser[a], Simon Musall[a,c*], and Viviana Rincón Montes[a*]

[a] Institute of Biological Information Processing (IBI-3) – Bioelectronics, *Forschungszentrum* Jülich, Germany

† Former member of IBI-3 and University of Konstanz

[b] Helmholtz Nano Facility (HNF), *Forschungszentrum* Jülich, Germany

[c] RWTH Aachen University, Germany

[d] JARA BRAIN Institute of Neuroscience and Medicine (INM-10), *Forschungszentrum Jülich*, Germany

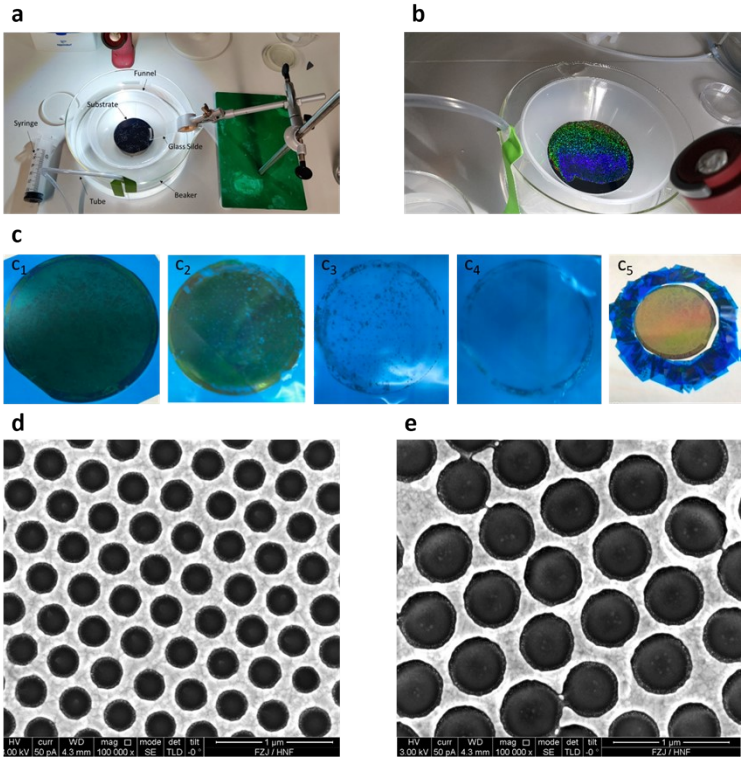

Figure S1. Fabrication of m-µECOGs. a) Funnel-assisted self-assembly setup. We poured the PSNPs dispersion onto the tilted wet glass slide until achieving a homogenous milky interface. Afterwards, we drained the water by applying negative pressure through a syringe; so that the water-air interface traps PSNPs. b) We confirmed the formation of the monolayer when shining light onto the substrate, which exhibited colourful shimmering according to the size of PSNPs. c) Lift-off process of PSNPs using dicing tape. We first placed carefully dicing tape onto the substrate, avoiding bubbles (c_1). To remove the PSNPs, we lifted the tape for at least three rounds until no NPs were observed on the tape ($c_2 - c_4$). To avoid rupturing the flexible PaC layer with the Au mesh structure, we also carried out the lift-off of PSNPs using smaller pieces of dicing tape, with the disadvantage that the process becomes more time-consuming. Scanning electron microscopy (SEM) images for the metal mesh structures (d and e). d) Metal mesh structure after etching 4 min 30 s during PSNP size reduction step with a lattice constant of 390 nm. e) Metal mesh structure after etching 6 min 30s during PSNP size reduction step with a lattice constant of 617 nm.

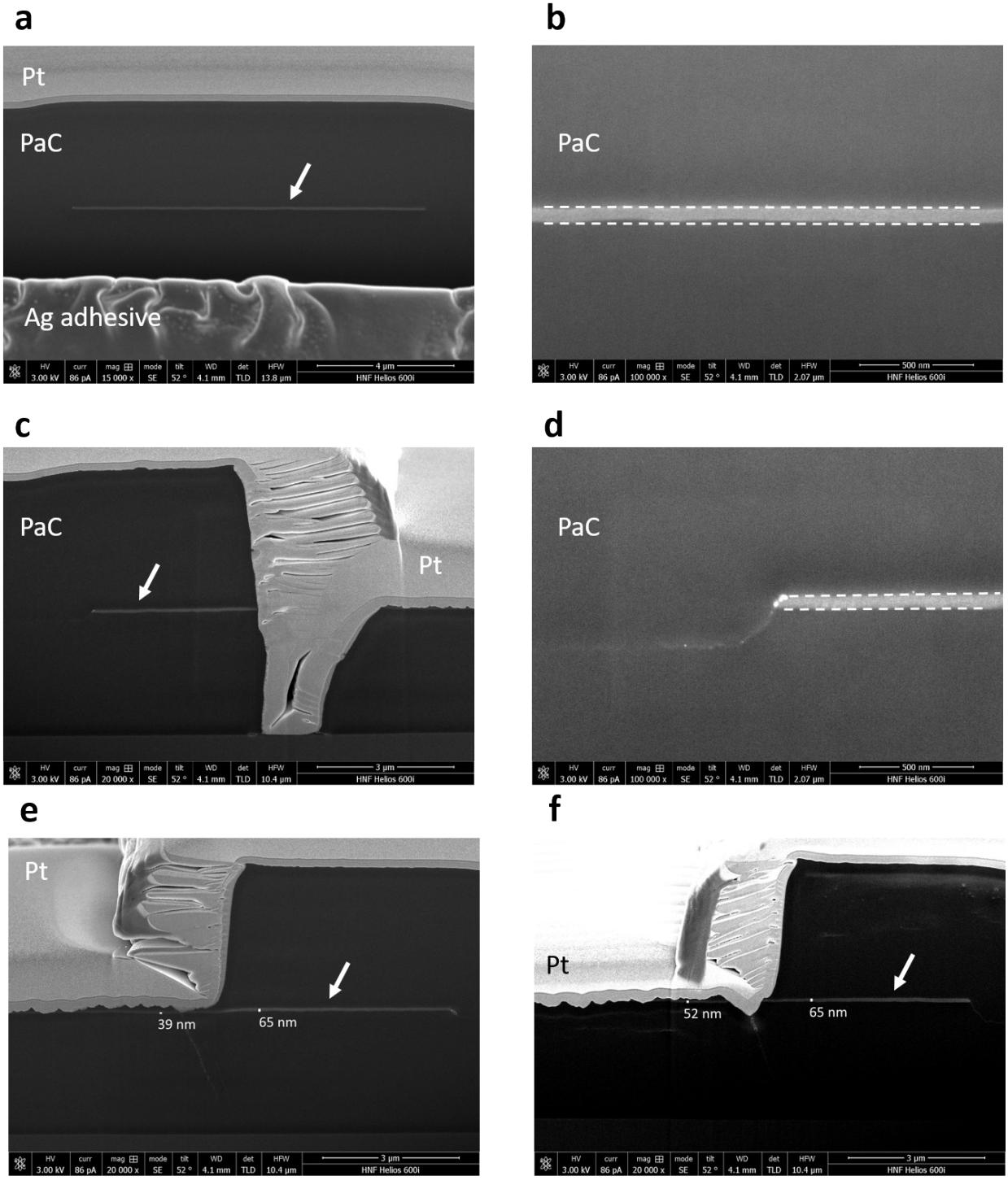

Figure S2. Focused-ion beam (FIB) cuts of spin-coated PEDOT: PSS layers. a) Exemplary FIB cut of a PEDOT: PSS feedline (white arrow) embedded in parylene-C (PaC). b) Close-up of (a) showing a PEDOT: PSS layer with an average thickness of 77 ± 2 nm (N = 6). c) Exemplary FIB cut of a PEDOT: PSS electrode (white arrow) embedded in PaC. d) Close-up (c) showing a PEDOT.PSS layer with an average thickness of 79 ± 8 nm (N = 10). Exemplary close-up of PEDOT: PSS electrodes without PaC passivation layer exposing a thickness of 39 nm (e) and 52 nm (f). White arrows point out the PEDOT:PSS layer.

Material	$R_{feedline}$ [kΩ]	$Z_{50\,\mu m}$ @ 1KHz [kΩ]
sAu	0.13	426
mAu	0.14	407
PP	107.76	15

Table S1. Lead resistance and impedance comparison across materials. We calculated the resistance of a feedline ($R_{feedline}$) and the impedance ($Z_{50\mu m}$ @ 1kHz) of an electrode with the dimensions used in this work considering three base materials: solid Au (sAu), mesh Au (mAu), and PEDOT: PSS (PP). For the calculation of $R_{feedline}$, the feedline length (comprising contact pad area and cable length) was 10.5 mm, and the width was 30 µm. The mean conductivity (σ) for each material (Figure 2c) was considered for the calculations. Therefore, σ_{sAu} = 229,500 S/cm; σ_{mAu} = 27,767 S/cm; σ_{PP} = 406 S/cm). Thicknesses of 110 nm, 120 nm, and 80 nm were used for sAu and mAu, and PP, respectively. We calculated $Z_{50\mu m}$ @ 1kHz for an electrode with a diameter of 50 µm and considered the extended Stern model as described in the section of Materials and Methods.

a

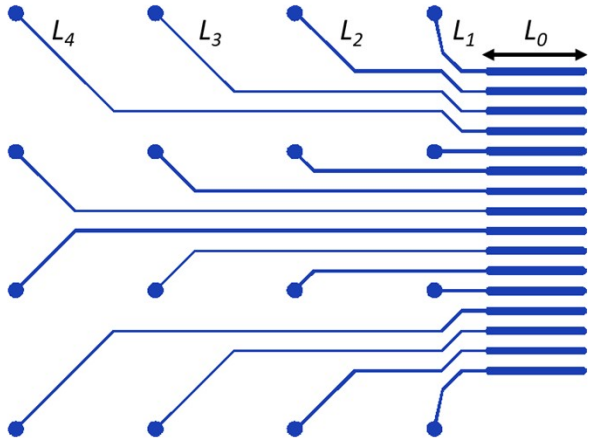

b

Length [µm] -width [µm]				
L_0 - w	L_1 - w	L_2 - w	L_3 - w	L_4 - w
400-30	326-10	854-10	1442-10	2031-10
$R_{feedline}$ [kΩ]				
4	10	26	44	63

Figure S3. Lead resistance of PEDOT: PSS-based feedlines. a) pp-µECoG design showing the feedlines and electrodes based on PEDOT:PSS. b) Top row: Length L_n [µm], width w [µm]. Bottom row: Lead resistance ($R_{feedline}$) calculation for each feedline component, considering a PEDOT: PSS thickness of 80 nm and a conductivity of 406 S/cm.

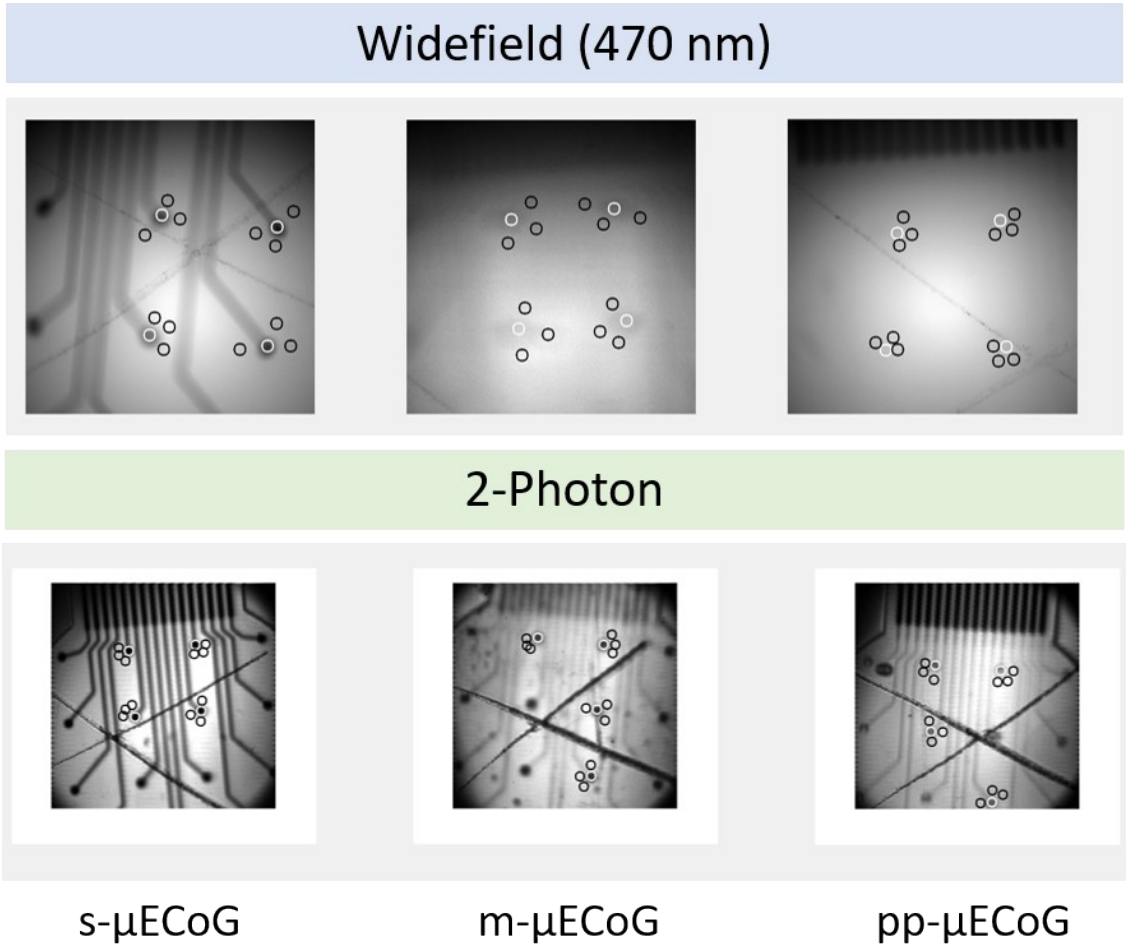

Figure S4. Example of electrode and background selection for electrode shadow quantification. Exemplary widefield and two-photon pictures for each implant type. White and black circles mark the regions of interest for selection of the electrode and background areas, respectively.

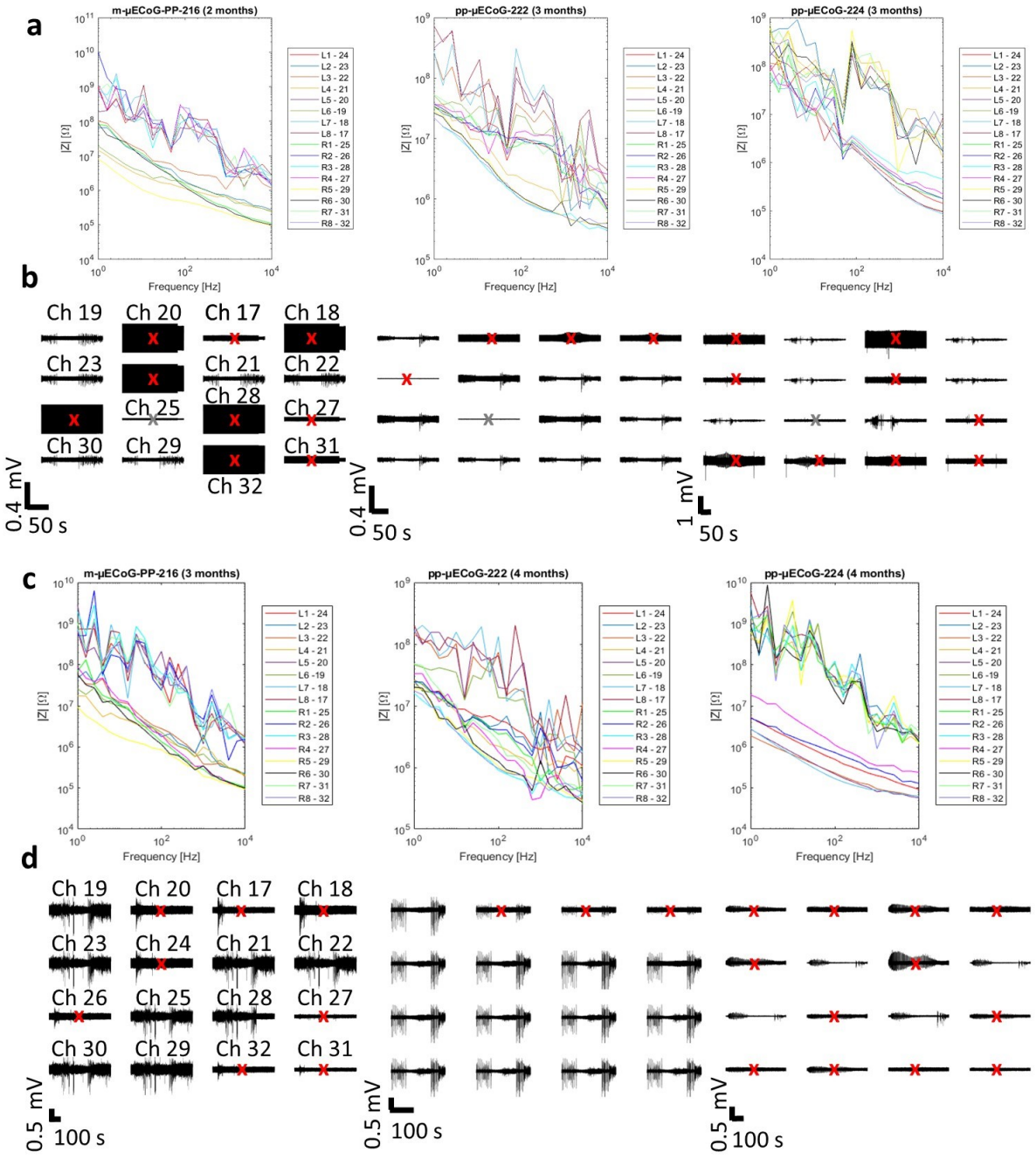

Figure S5. Chronic implantation performance. a) *In vivo* impedance spectra and b) overview of electrophysiological signals captured during anaesthesia test two- and three-months post-implantation for m-µECoG-PP (left column) and pp-µECoGs (middle and right column), respectively. Non-working electrodes are marked with a red cross, matching the electrodes that exhibited high impedances in (a). A broken pin in the headstage is marked in grey. Correlating impedance with electrophysiology, m-µECoG-PP-216, pp-µECoG-222, and pp-µECoG224 exhibited 43% (7/16), 75% (12/16), and 43% (7/16) working electrodes upon chronic implantation, respectively. c) and d) same as in a) and b) but after three and four months of chronic implantation. Correlating impedance with electrophysiology, m-µECoG-PP-216, pp-µECoG-222, and pp-µECoG224 exhibited 50% (8/16), 80% (13/16), and 25% (4/16) working electrodes upon chronic implantation, respectively.

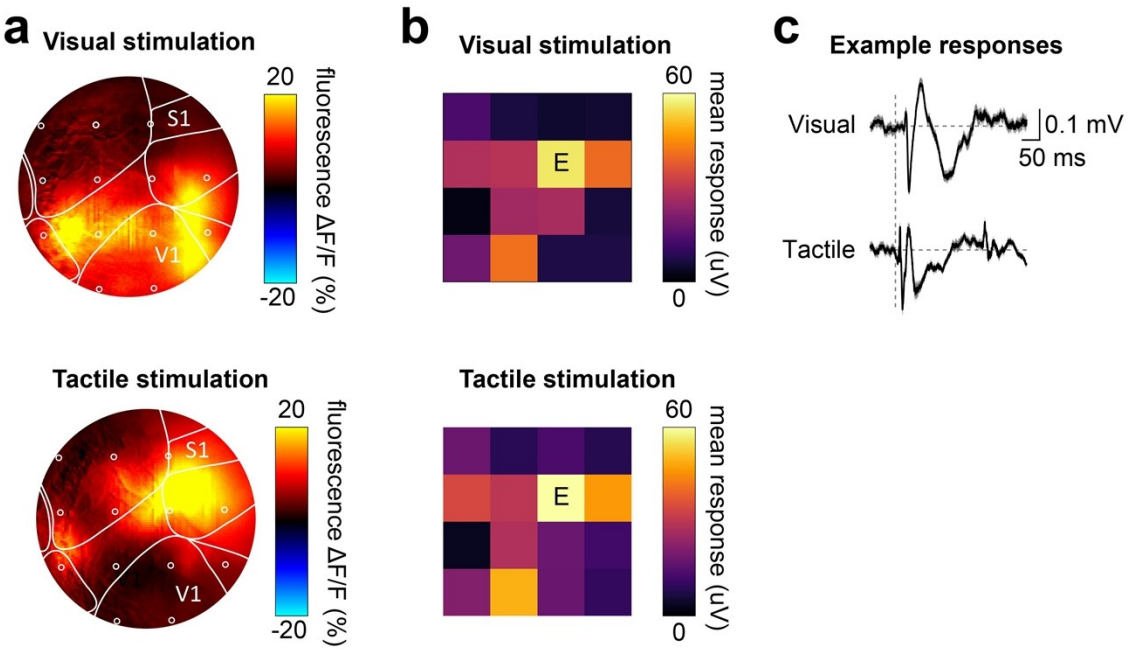

Figure S6. Widefield imaging functionality of m-µECoG-PP. a) m-µECoG-PP was chronically implanted over V1 and S1 cortex of a GCaMP6s-expressing mouse. White lines show borders of different cortical areas. Functional maps show changes in fluorescence signals during widefield imaging in response to either visual (top) or tactile stimulation (bottom). Images show average responses of over 75 stimulus presentations. White circles indicate the location of the recording electrodes. b) Average event-related potentials as measured with the m-µECoG array. Matrices show the mean response magnitude within 100 ms after stimulus presentation. c) Traces show example recordings from electrodes E with clear responses to tactile or visual stimulation. Shading shows standard deviation across trials.

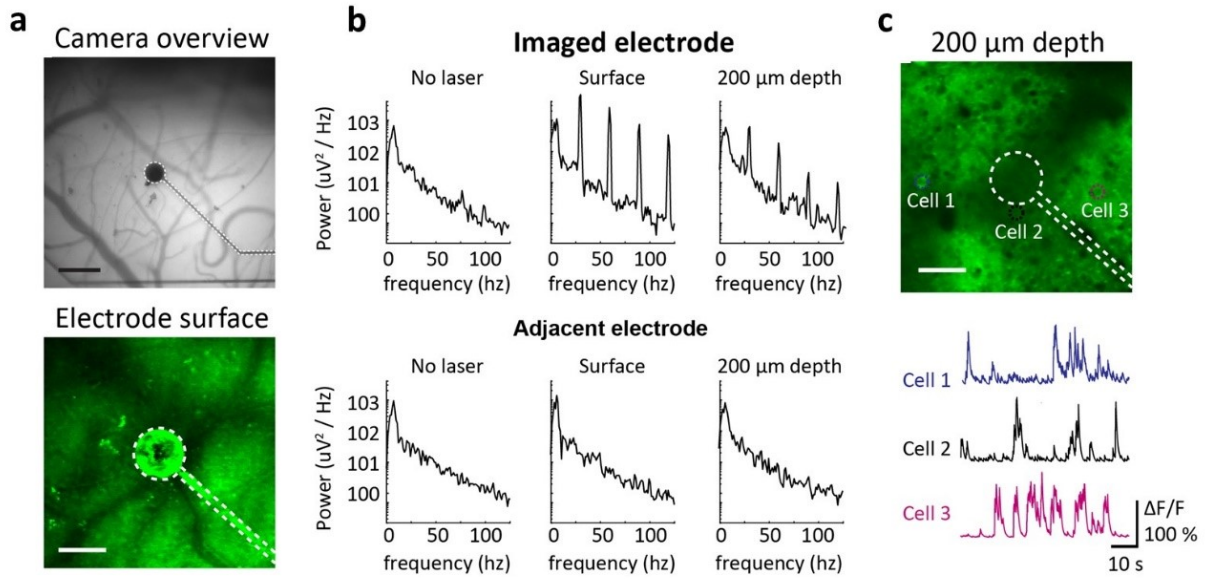

Figure S7. Two-photon functionality m-µECoG-PP. a) Fluorescent vessel image of a chronically implanted m-µECoG electrode over somatosensory cortex. Black dashed lines indicate the location of the transparent electrode. Scale bar = 100 µm. Bottom: Two-photon image of the same electrode as in the top image. Scale bar = 50 µm. b) Power spectral density of the electrode shown in a) and an adjacent electrode during different stages of imaging. Spectra on the left were taken before imaging was started, spectra in the middle while focusing the laser directly on the electrode, and spectra on the right while imaging 200 µm below the electrode. c) Same imaging location as the bottom image in a) but focused 200 µm below the electrode. Dashed circles indicate the location of 3 example cells for which functional signals are shown below. Cell 2 was imaged directly below the electrode.